Metal Ion-Coordinating Properties in Aqueous Solution of the Antivirally Active Nucleotide Analogue (*S*)-9-[3-Hydroxy-2-(phosphonomethoxy)propyl]adenine (HPMPA). Quantification of Complex Isomeric Equilibria

Claudia A. Blindauer,[a,b] Antonín Holý,†[c] Bert P. Operschall,[a] Astrid Sigel,[a] Bin Song,[a,d] and Helmut Sigel*[a]

Keywords: Acyclic nucleoside phosphonates · Antivirals · Isomeric equilibria · Metal ion complexes · Nucleotide analogues

---

[a] *Department of Chemistry, Inorganic Chemistry, University of Basel, Spitalstrasse 51, CH-4056 Basel, Switzerland*
E-mail: Helmut.Sigel@unibas.ch
www.chemie1.unibas.ch/~sigel/index.html

[b] *Department of Chemistry, University of Warwick, Coventry CV4 7AL, UK*
E-mail: C.Blindauer@warwick.ac.uk

[c] *Institute of Organic Chemistry and Biochemistry, Centre of Novel Antivirals and Antineoplastics, Academy of Sciences, CZ-16610 Prague, Czech Republic*

[d] *Vertex Pharmaceuticals Inc., 50 Northern Avenue, Boston, MA 02210, USA*

† *Deceased*

DOI: 10.1002/ejic.201900620

Abstract: Acyclic nucleoside phosphonates are of medical relevance and deserve detailed chemical characterization. We focus here on (*S*)-9-[3-hydroxy-2-(phosphonomethoxy)propyl]adenine (HPMPA) and include for comparison 9-[2-(phosphonomethoxy)ethyl]adenine (PMEA), as well as the nucleobase-free (phosphonomethoxy)ethane (PME) and (*R*)-hydroxy-2-(phosphonomethoxy)propane (HPMP). The acidity constants of $H_3(HPMPA)^+$ were determined and compared with those of the related phosph(on)ate derivatives; they are also needed to understand the properties of the metal ion complexes. Given that *in vivo* nucleotides and their analogues participate in reactions typically as divalent metal ion (M^{2+}) complexes, the stability constants of the $M(H;HPMPA)^+$ and M(HPMPA) species with $M^{2+} = Mg^{2+}$, Ca^{2+}, Sr^{2+}, Ba^{2+}, Mn^{2+}, Co^{2+}, Ni^{2+}, Cu^{2+}, Zn^{2+}, and Cd^{2+} were measured. Comparisons between the results for $HPMPA^{2-}$ and the previous data for $PMEA^{2-}$, $HPMP^{2-}$ and PME^{2-} revealed that for most M(HPMPA) complexes the enhanced stability (the enhancement relative to the stability of a simple phosphonate-M^{2+} coordination), can solely be explained by the formation of 5-membered chelates involving the ether oxygen. These chelates occur in equilibrium with simple 'open' phosphonate-M^{2+} species, the phosphonate group being the primary binding site. The only exceptions are the M(HPMPA) complexes of Ni^{2+}, Cu^{2+}, and Zn^{2+}, which show an additional stability enhancement; in these instances not only the indicated 5-membered chelates are formed, but M^{2+} coordinates in addition to N3 of the adenine residue forming a 7-membered chelate ring. This observation regarding N3 is important because it emphasizes the metal ion affinity of this site (which is often ignored). Note that in the DNA double helix N3 is exposed to the solvent in the minor groove. The stability data for the monoprotonated $M(H;HPMPA)^+$ complexes suggest that these carry H^+ at the phosphonate group whereas M^{2+} is partly at the nucleobase and partly also at the phosphonate group. The ratios of these isomers depend on the metal ion involved, e.g., for Cu(H;HPMPA) the ratio of the isomers is about 1:1.

1. Introduction

Acyclic nucleoside phosphonates (ANPs) and their derivatives are a highly successful class of antiviral compounds.[1,2] The first ANP to be synthesized and evaluated for its antiviral activity was (*S*)-9-[3-hydroxy-2-(phosphonomethoxy)propyl]adenine [(*S*)-HPMPA] in 1986.[3] This compound is derived from the acyclic adenosine analogue [(*S*)-9-(2,3-dihydroxypropyl)adenine],[4] which has been commercialized in the Czech Republic as Duviragel against Herpes simplex virus.

Although (*S*)-HPMPA showed impressive activities against a range of DNA viruses,[3] it was never commercialized as a drug. However, it spawned three immensely successful drug molecules, namely (*S*)-9-[3-hydroxy-2-phosphonomethoxy)propyl]cytosine [(*S*)-HPMPC; Cidofovir]; 9-[2-(phosphonomethoxy)ethyl]adenine) (PMEA; Adefovir), and (*R*)-9-[2-(phosphonomethoxy)propyl]adenine) [(*R*)-PMPA; Tenofovir].[1,2] HPMPC differs from HPMPA by replacement of the nucleobase, PMEA lacks a hydroxymethyl group, and PMPA lacks the 3-hydroxyl group present in HPMPA (Figure 1, *vide infra*). With a similar broadband antiviral spectrum as HPMPA, Cidofovir (HPMPC) attained FDA (1996) and EMA (1997) approval, under the tradename Vistide, for the treatment of human cytomegalovirus retinitis in AIDS patients.[5] Cidofovir (now generic) remains in use for a variety of viral infections.[1] Furthermore, the oral prodrug Brincidofovir, the hexadecyloxypropyl ester of HPMPC has been given orphan designation for treatment of smallpox.[6] Since 2003, Adefovir (PMEA) is in use in the form of its orally available bis(pivaloyloxymethyl) ester, Adefovir dipivoxil (Hepsera), for the treatment of hepatitis B virus infections.[7] Tenofovir (PMPA) is available since 2002 as an oral prodrug, Tenofovir disoproxil fumarate (TDF, Viread), against infections with HIV-1.[8] TDF is a component of several combination regimens, including Truvada which can prevent HIV-1 infections.[9]

(*S*)-HPMPA does not only display antiviral activity, but has also been considered for the treatment of Schistosomiasis that is caused by a flatworm,[10] Malaria caused by the unicellular parasite *Plasmodium falciparum*,[11] and for combating infections with the protozoon *Trypanosoma brucei* which causes sleeping sickness.[12] In addition, it exhibits

immunobiological activity, leading to the activation of macrophages.[13] It also remains in the focus of antiviral research; in particular, a range of oral prodrugs have been investigated,[14-17] most recently with a view to combat adenovirus infections that are otherwise difficult to tackle.[18,19]

insert Figure 1 close to here

The mechanistic details for the activity of ANPs against viruses are relatively well studied.[20] ANPs are essentially isosteric analogues of the respective (2'-deoxy)nucleoside 5'-monophosphates (5'-NMPs) such as 5'-(d)AMP^{2-} (Figure 1).[21–27] Owing to their fairly polar character and charge(s) on the phosphonate group, unmodified ANPs need to be administered by injection, and are thought to be taken up into cells by endocytosis,[28] whereas the esterified oral prodrugs may permeate through cell membranes,[20] and are then de-esterified by phospholipase C or phosphodiesterase.[20] Free phosphonates are successively phosphorylated by cellular kinases; action of AMP/dAMP kinase on HPMPA yields its diphosphorylated derivative HPMPApp^{4-}.[29,30] Such (2'-deoxy)nucleoside 5'-triphosphate [(d)NTP^{4-}] analogues serve as alternative substrates and effective competitive inhibitors of nucleic acid polymerases.[30] In addition, strands harbouring a single HPMP derivative are inefficient templates for further nucleic acid synthesis.[31] Summarily, these actions inhibit the replication of the viral genome and hence virus proliferation.

The phosphonate group is a cornerstone for the clinical success of the ANPs.[32] It circumvents the requirement for a nucleoside kinase, and in contrast to a hydrolysable phosphate ester group, it avoids degradation and inactivation by phosphatases and esterases.[33] Moreover, after incorporation of the ANP into the growing nucleic acid strand, it also prevents the excision of the ANP by proof-reading polymerases.[20]

Since the substrates for kinases and nucleic acid polymerases are actually metal complexes of the respective nucleoside mono- or triphosphates,[34–37] it is conceivable that the metal ion-binding properties of ANPs may also play a role in the activity of these compounds, motivating a research programme dedicated to understanding stability and structures of ANP metal complexes.[35,38,39] The ether oxygen has been shown to be essential for biological activity[40,41] but also to play a pivotal role in metal ion binding of these compounds: It permits the formation

of five-membered chelates.[38,42–47] Finally, in terms of biological activity, the position of the hydroxyl group matters, as "iso-HPMPA", (*S*)-9-[2-hydroxy-2-(phosphonomethoxy)propyl]adenine), is inactive.[48]

Summarily, the groups that are critical to the metal ion-binding properties of ANPs also influence the suitability of the ANPs as enzyme substrates. In the present study, we investigate the metal ion-binding properties of $H(HPMPA)^-$ and $HPMPA^{2-}$ which will allow comparisons with its congener PMEA species. Previously HPMPA had been used as a ligand in aqueous solution in two studies: Most recently the stability and structure of the ternary Cu(Arm)(H;HPMPA)$^+$ and Cu(Arm)(HPMPA) complexes, where Arm = 2,2'-bipyridine or 1,10-phenanthroline, were examined.[39] The binary $H(HPMPA)^-$ and $HPMPA^{2-}$ systems with Ca^{2+}, Cu^{2+}, and Zn^{2+} were investigated previously in a preliminary study and these results were confirmed now.[49] With comparative data for the nucleobase-free parent compound HPMP now available,[47] it has become possible to comprehensively evaluate the stability constants of the binary M(H;HPMPA)$^+$ and M(HPMPA) complexes, formed with $M^{2+} = Mg^{2+}$, Ca^{2+}, Sr^{2+}, Ba^{2+}, Mn^{2+}, Co^{2+}, Ni^{2+}, Cu^{2+}, Zn^{2+}, and Cd^{2+}, and to assess their structures in solution revealing in part up to three different isomeric species, including N3 as a binding site.

2. Results and Discussion

Nucleobases, especially purines, and their derivatives can undergo self-associations via π stacking.[23,50–52] Therefore, the experimental conditions for the determination of the stability constants of the M(H;HPMPA)$^+$ and M(HPMPA) complexes by potentiometric pH titrations in aqueous solution were selected such that the results refer to monomeric species (see 4. Experimental Section). With ligand concentrations of 0.3 mM, this is ascertained as shown previously for PMEA.[38] These statements[44,52] as well as the contents of Sections 2.1, 2.2, and 2.3 are partially analogous to previous related studies.[43,44,46,52]

2.1 Acidity Constants of $H_3(HPMPA)^+$ and of Related Species

$HPMPA^{2-}$, like $PMEA^{2-}$,[21] can accept three protons, two at the phosphonate group and one at the N1 site of the purine residue. Further protonations are possible at N7 and N3, but these protons are released[53] with $pK_a < 0$ and are thus not of relevance here, though as metal ion-binding sites they may be relevant [see Sections 2.4, 2.5 (N1, N7) and 2.6, 2.7 (N3, N7)]. At pH > 0, the strongest acid that exists in aqueous solution based on $HPMPA^{2-}$ is $H_3(HPMPA)^+$. The corresponding three deprotonation steps, written in a general manner, where NP^{2-} = nucleoside phosph(on)ate (see Figure 1), are the following ones:

$$H_3(NP)^+ \rightleftharpoons H_2(NP)^{\pm} + H^+ \quad (1a)$$

$$K^{H}_{H_3(NP)} = [H_2(NP)^{\pm}][H^+]/[H_3(NP)^+] \quad (1b)$$

$$H_2(NP)^{\pm} \rightleftharpoons H(NP)^- + H^+ \quad (2a)$$

$$K^{H}_{H_2(NP)} = [H(NP)^-][H^+]/[H_2(NP)^{\pm}] \quad (2b)$$

$$H(NP)^- \rightleftharpoons NP^{2-} + H^+ \quad (3a)$$

$$K^{H}_{H(NP)} = [NP^{2-}][H^+]/[H(NP)^-] \quad (3b)$$

insert Table 1 close to here

The acidity constants for $H_3(HPMPA)^+$ are listed in Table 1 together with related data.[53–64] From the assembled constants the following conclusions, next to others, are possible:

(1) The protons of $H_3(HPMPA)^+$ are released from the acidic sites in the order $P(O)(OH)_2 > (N1)H^+ > PO_2^-(OH)$ (entry 3).

(2) The given order is confirmed by entries 1 to 3 and it also holds for $H_3(PMEA)^+$ (entry 5).

(3) The $P(O)(OH)_2$ group of the nucleobase-free compounds $H_2(HPMP)$ and $H_2(PME)$ is somewhat less acidic than the corresponding group of $H_3(HPMPA)^+$ and $H_3(PMEA)^+$ (Δ pK_a ca. 0.35). The reason is that the repulsive effect of $(N1)H^+$ is missing.

(4) The site attribution for $H_3(AMP)^+$ (entry 8) follows from entries 1, 6, and 7, and it is analogous to that of $H_3(HPMPA)^+$ and $H_3(PMEA)^+$.

(5) The phosphate derivatives are more acidic than the phosphonate ones. This is

especially evident for $P(O)(OH)_2^-$ of methyl phosphate (entry 9) and methylphosphonate (entry 10) (Δ pK_a ca. 1.15).

(6) The consequence of point (5) is that at the physiological pH of 7.5 about 50% of methylphosphonate exist in its monoprotonated form, whereas for methyl phosphate this is the case for only about 7%. Consequently, at physiological pH there is less proton competition regarding metal ion binding with phosphate monoesters than there is for phosphonates.

(7) A final point to be emphasized is that in adenine derivatives with a free N1 site, N7 possesses a considerable basicity (column 4 of Table 1). This is of relevance for macrochelate formation, e.g., in M(AMP) complexes.[56,57,65–68]

2.2 Stability Constants of the M(H;HPMPA)$^+$ and M(HPMPA) Complexes

The experimental data of potentiometric pH titrations (see 4. Experimental Section) allow the determination of the stability constants according to Equilibria (4a) and (5a), which are written in a general manner with NP^{2-} = $HPMPA^{2-}$. It should be noted that in formulae like $M(H;NP)^+$, the H^+ and NP^{2-} are separated by a semicolon to facilitate reading, yet they appear within the same parenthesis to indicate that the proton is at the ligand without defining its location:[46]

$$M^{2+} + H(NP)^- \rightleftharpoons M(H;NP)^+ \quad (4a)$$

$$K^M_{M(H;NP)} = [M(H;NP)^+]/([M^{2+}][H(NP)^-]) \quad (4b)$$

$$M^{2+} + NP^{2-} \rightleftharpoons M(NP) \quad (5a)$$

$$K^M_{M(NP)} = [M(NP)]/([M^{2+}][NP^{2-}]) \quad (5b)$$

For the M^{2+}/HPMPA system, Equilibria (2a), (3a), (4a), and (5a) are sufficient to obtain an excellent fitting of the titration data provided that the evaluation is not carried into the pH range where the formation of hydroxo species occurs; this was evident from the titrations without the ligand (4. Experimental Section).[46]

Naturally, Equilibria (4a) and (5a) are also connected *via* Equilibrium (6a):

$$M(H;NP)^{+} \rightleftharpoons M(NP) + H^{+} \quad (6a)$$

$$K^{H}_{M(H;NP)} = [M(NP)][H^{+}]/[M(H;NP)^{+}] \quad (6b)$$

The corresponding acidity constant [Eq. (6b)] may be calculated with Equation (7):

$$pK^{H}_{M(H;NP)} = pK^{H}_{H(NP)} + \log K^{M}_{M(H;NP)} - \log K^{M}_{M(NP)} \quad (7)$$

The results are listed in Table 2. The stability constants given for the $M(H;NP)^{+}$ complexes carry, in part, rather large error limits because the formation degree of these species was low.

insert Table 2 close to here

The stability constants of the $M(H;HPMPA)^{+}$ complexes reflect the Irving-Williams sequence[69] and this might be taken as a hint that (N)–M^{2+}-binding, that is, involvement of the nucleobase residue, is of some relevance.[70]

In contrast, the stability constants of the M(HPMPA) complexes with the 3d metal ions confirm the long-standing experience[70] that the stabilities of phosph(on)ate-metal ion complexes often do not strictly follow[57,66,71,72] the Irving-Williams sequence.[69] This observation agrees with the fact that in ligands of this kind the phosph(on)ate group is generally[35,66,67,71,73,74] the main stability-determining binding site (see Figure 3, *vide infra*). For the alkaline earth ions, complex stability decreases (Table 2, column 3), as one might expect, with increasing ionic radii, thus indicating that M^{2+} binding at the phosphonate group occurs at least partly innersphere.

2.3 Where Is the Proton in the Monoprotonated M(H;HPMPA) Species?

The evaluation of potentiometric pH titration data only allows the determination of the stability constants of the $M(H;HPMPA)^{+}$ complexes. Further information is required to detect the binding sites of the proton and the metal ion.[46,47,75,76]

Regarding the location of the proton it is helpful to consider the deprotonation Equilibrium (6a). The corresponding acidity constant follows from Equation (7) and these results are listed in

column 4 of Table 2. The values for these acidity constants, $pK^{H}_{M(H;HPMPA)}$, are all in the pK_a range of about 4.58 (± 0.22) to 5.5 (± 0.5). This means, these values are about 0.44 (± 0.22) to 1.4 (± 0.5) pK units above the pK_a value of the adenine nucleobase ($pK^{H}_{(N1)H} = pK^{H}_{H_2(HPMPA)} =$ 4.14 ± 0.01; Table 1, entry 3), but below $pK^{H}_{P(O)_2(OH)} = pK^{H}_{H(HPMPA)} = 6.84 \pm 0.01$.

The above observation allows to conclude that the proton in these $(M;HPMPA)^+$ complexes resides at the phosphonate group, and that the presence of M^{2+} increases the acidity of the $P(O)_2^-(OH)$ group by about 1.3 (± 0.5) to 2.26 (± 0.22) pK units.

2.4 Where Is the Metal Ion Coordinated in the Monoprotonated $M(H;HPMPA)^+$ Complexes?

In the second to the last paragraph of Section 2.2 a hint is given for a (N)–M^{2+} binding, that is, for a M^{2+}-adenine residue interaction, and in the preceding Section 2.3 it was concluded that in the monoprotonated $M(H;HPMPA)^+$ complexes the proton is located at the phosphonate group of $HPMPA^{2-}$. Hence, the formation of the monoprotonated $M(H;HPMPA)^+$ complexes can occur in two ways: That is, M^{2+} coordinates at the nucleobase with the proton at the phosphonate group, this species being represented by the expression $(H{\cdot}HPMPA{\cdot}M)^+$, or the other possibility is that both the proton and the metal ion are located at the phosphonate group; this species is written as $(H{\cdot}M{\cdot}HPMPA)^+$, though one might imagine that the M^{2+} ion at the phosphonate interacts to some extent also with the adenine residue forming a macrochelate as expressed by $(H{\cdot}HPMP{\cdot}M{\cdot}A)^+$. These two species with M^{2+} at the phosphonate group we consider together under the label $H(M{\cdot}HPMPA)^+$. The existence of a further species with the metal ion at the phosphonate group and the proton at the N1 site is rather unlikely because in the uncomplexed species $(H{\cdot}HPMPA{\cdot}H)^{+/-}$ the pK_a of the $(N1)H^+$ site is 4.14 (Table 1, entry 3, column 5) and for $(M{\cdot}HPMPA{\cdot}H)^+$ it will be similar or even lower and an isomer with such a low pK_a value is expected not to be of a significant relevance in the context of the other isomers formed (*vide infra* Table 4, columns 5 and 6).

At this point we are left with $(H{\cdot}HPMPA{\cdot}M)^+$ and $H(M{\cdot}HPMPA)^+$, and these two

possibilities are summarized in Figure 2 where the metal ion at the adenine residue (with Ni^{2+} as an example) is given in the upper pathway. The isomers with M^{2+} at the phosphonate group, if chelated or not, are indicated as $H(M{\cdot}HPMPA)^{+}$.

insert Figure 2 close to here

Both protonated species lead after deprotonation to the same complex, M(HPMPA), which is shown in the equilibrium scheme of Figure 2 at the right. By determining the micro stability constants of the $(H{\cdot}HPMPA{\cdot}M)^{+}$ and $H(M{\cdot}HPMPA)^{+}$ species one may evaluate which of the two pathways is the dominating one. The interrelations between the macroconstants and the microconstants, which appear in the scheme, are given in the lower part of Figure 2.

From Figure 2 it follows that there are four unknown microconstants but only three equations which interrelate these micro- with the experimentally accessible macroconstants. Hence, one of the microconstants needs to be obtained in an independent manner. From the structures shown in Figure 1 it is evident that the adenine moiety of adenosine (Ado) is a good mimic of the corresponding residue of $H(HPMPA)^{-}$. Certainly, the corresponding two metal ion complexes $M(Ado)^{2+}$ and $M(H;HPMPA)^{+}$ differ by a charge of one and this needs to be taken into account in the evaluations.

There is also a difference in the basicity of N1 in Ado compared with that in $H(HPMPA)^{-}$ which is reflected in the corresponding acidity constants. For $H_2(HPMPA)^{+/-}$ it holds $pK^{H}_{H_2(HPMPA)} = 4.14 \pm 0.01$ (Table 1) and for $H(Ado)^{+}$ $pK^{H}_{H(Ado)} = 3.61 \pm 0.03$, a value which shows no marked dependence on the ionic strength between $I = 0.1$ and 0.5 M (Table 1).[27] The difference in acidity as expressed in Equation (8)

$$\Delta\, pK_a = (4.14 \pm 0.01) - (3.61 \pm 0.03) = 0.53 \pm 0.03 \qquad (8)$$

is expected (due to the known dependence of log $K_{stability}$ on pK_a) to be reflected in the metal ion-binding strength of the adenine residue. The straight-line plots of *o*-substituted pyridine-type ligands reflect metal ion binding at N1,[77] whereas the plots of 1-methyl-4-aminobenzimidazole-type (= 9-methyl-1,3-dideazaadenine) or 1,4-dimethylbenzimidazole-type (= 6,9-dimethyl-1,3-dideazapurine) ligands reflect the metal ion affinity of the N7 side.[78] As the dichotomy for metal-ion binding, especially between N1 and N7 is well known,[79] we used the average of the

slopes *m* of the two straight-line plots (Table 3, column 2) as the best available slope, m_{av}, for the dependence of the N1,N7-metal ion affinity. As the contribution of the term $m_{av} \cdot \Delta\ pK_a$ is small, no significant error is introduced by this procedure.

If one summarizes the various terms indicated above, one obtains an estimate for the micro stability constant of the $(H \cdot HPMPA \cdot M)^+$ isomer. This is expressed in Equation (9):

$$\log\ K^{M}_{M(Ado)} + m_{av} \cdot \Delta\ pK_a + \text{charge effect} = \log\ k^{M}_{H \cdot HPMPA \cdot M} \qquad (9a)$$

$$\log\ K^{M}_{M(Ado)} + m_{av} \cdot (0.53 \pm 0.03) + (0.40 \pm 0.15) = \log\ k^{M}_{H \cdot HPMPA \cdot M} \qquad (9b)$$

The charge effect results from the negative charge of the $P(O)_2^-(OH)$ group on the metal ion affinity of the adenine residue. We applied a charge effect of 0.40 ± 0.15 log units with a relatively large error limit; its size has been repeatedly confirmed.[38,56,59,80] The corresponding results are summarized in Table 3.[80–82] The complexes of the alkaline earth ions are not considered because the stabilities of the corresponding $M(H;HPMPA)^+$ (Table 2) and $M(Ado)^{2+}$ (ref.[81]) species are very low and the error limits are thus large.

insert Table 3 close to here

The information assembled in Table 3 allows, in combination with the stability constants listed in Table 2, the calculation of the microconstants defined in Figure 2. The corresponding micro stability as well as the micro acidity constants are summarized in Table 4. The micro acidity constants are of special interest because one would expect that a metal ion coordinated at the adenine residue will enhance the acidity of a proton at the phosphonate group less than a metal ion that is coordinated next to the proton also at the phosphonate group. Therefore, from the observation that for the Mn^{2+}, Co^{2+}, and Cd^{2+} complexes it holds $pk^{H}_{H \cdot HPMPA \cdot M} > pk^{H}_{H(M \cdot HPMPA)}$, it follows that in these instances the isomer with the metal ion at the nucleobase residue dominates. The micro acidity constants indicate further that for the complex with Zn^{2+} the reverse is true, that is, the lower pathway in Figure 2 dominates demonstrating that matters can be more complicated. For the Ni^{2+} and Cu^{2+} complexes the two micro acidity constants are rather similar indicating an approximately even formation degree of the two species with M^{2+} at the adenine residue or at the phosphonate group. Indeed, these indications are confirmed below.

insert Table 4 close to here

2.5 Attempt to Determine the Formation Degrees of the M(H;HPMPA)$^+$ Isomers

Naturally, at this point one wonders about the position of the intramolecular equilibrium between the two isomeric species (H·HPMPA·M)$^+$ and H(M·HPMPA)$^+$ seen in the equilibrium scheme in Figure 2. This position is defined by the dimension-less intramolecular equilibrium constant K_I which corresponds to the ratio R of these species; R is defined by Equation (10):

$$R = \frac{[(\mathrm{H}\cdot\mathrm{HPMPA}\cdot\mathrm{M})^+]}{[\mathrm{H}(\mathrm{M}\cdot\mathrm{HPMPA})^+]} = \frac{k^{\mathrm{M}}_{\mathrm{H}\cdot\mathrm{HPMPA}\cdot\mathrm{M}}}{k^{\mathrm{M}}_{\mathrm{H}(\mathrm{M}\cdot\mathrm{HPMPA})}} \qquad (10)$$

The two micro stability constants are interlinked with each other (see also the equilibrium scheme) by Equation (a) of Figure 2. Based on these equations and the information assembled in Tables 2 and 3 the ratio R can be calculated as well as the formation degree of the species in which M^{2+} is located at the nucleobase residue (Equation (11)):

$$\%\ (\mathrm{H}\cdot\mathrm{HPMPA}\cdot\mathrm{M})^+ = 100\cdot R/(1 + R) \qquad (11)$$

The corresponding results are provided in Table 5.

insert Table 5 close to here

Not surprisingly, the error limits of the results presented in Table 5 are large, however, it is still evident that both isomers occur in varying amounts. In addition, it is comforting to note that the interpretations given in the context of Table 4 are confirmed. Further interpretations are hampered by the large errors because for % (H·HPMPA·M)$^+$ the lower limits for Mn^{2+}, Co^{2+}, and Cd^{2+} overlap with the upper limits of Ni^{2+} and Cu^{2+}. The only value that is significantly different from all the others is 17±6 for % (H·HPMPA·Zn)$^+$. The reason for this observation is most likely that Zn^{2+} has a chameleon-like coordination sphere[83] and switches easily from an octahedral one to a tetrahedral one, that is, from coordination number 6 (via 5) to 4.[83] However, overall the observation that metal ions, without the support of any other binding site, can

coordinate to the adenine residue[79] (via N1 and/or N7)[84] is certainly of biological relevance. The same is true for the proof that H^+ and M^{2+} may simultaneously bind to a given phosph(on)ate group. Regarding metal ion coordination to phosphodiester units in oligonucleotides this is also of relevance.

2.6 Definition of the Stability Enhancements for M(NP) Complexes and Comparisons Among Structurally Related Species. Effects of Substituents

A stability enhancement for any ANP complex is observed, if the experimentally measured stability constant [Eq. (5)] is larger than the one expected based on a simple phosphonate-metal ion coordination. For the M(PMEA) complexes stability enhancements were found. Based on steric and chemical considerations,[35,74] which were confirmed by NMR studies,[85] it was concluded that the dominating pathway involves N3 and thus the upper pathway of the Equilibrium Scheme (12);[45] if at all, in the case of Ni^{2+} (ref.[86]) or Cu^{2+} (ref.[87]) only very low amounts of $M(PMEA)_{cl/N7}$ form (see also ref.[45]). For the case of Ni(HPMPA) or Cu(HPMPA) it is concluded that $M(NP)_{cl/N7}$ is not of relevance (see also below).

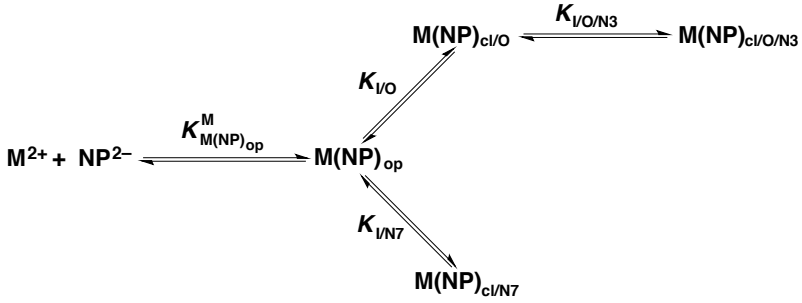

(12)

The three equilibrium constants of the upper part of the Equilibrium Scheme (12) are defined by Equations (13) to (15):

$$K^{M}_{M(NP)_{op}} = \frac{[M(NP)_{op}]}{[M^{2+}][NP^{2-}]} \tag{13}$$

$$K_{I/O} = \frac{[M(NP)_{cl/O}]}{[M(NP)_{op}]} \tag{14}$$

$$K_{\mathrm{I/O/N3}} = \frac{[\mathrm{M(NP)_{cl/O/N3}}]}{[\mathrm{M(NP)_{cl/O}}]} \tag{15}$$

With these definitions the measured overall stability constant [Eq. (5b)] can be redefined by Equations (16a) through (16d):

$$K^{\mathrm{M}}_{\mathrm{M(NP)}} = \frac{[\mathrm{M(NP)}]}{[\mathrm{M}^{2+}][\mathrm{NP}^{2-}]} \tag{16a}$$

$$= \frac{[\mathrm{M(NP)_{op}}] + [\mathrm{M(NP)_{cl/O}}] + [\mathrm{M(NP)_{cl/O/N3}}]}{[\mathrm{M}^{2+}][\mathrm{NP}^{2-}]} \tag{16b}$$

$$= K^{\mathrm{M}}_{\mathrm{M(NP)_{op}}} + K_{\mathrm{I/O}} \cdot K^{\mathrm{M}}_{\mathrm{M(NP)_{op}}} + K_{\mathrm{I/O/N3}} \cdot K_{\mathrm{I/O}} \cdot K^{\mathrm{M}}_{\mathrm{M(NP)_{op}}} \tag{16c}$$

$$= K^{\mathrm{M}}_{\mathrm{M(NP)_{op}}} (1 + K_{\mathrm{I/O}} + K_{\mathrm{I/O}} \cdot K_{\mathrm{I/O/N3}}) \tag{16d}$$

The connection between the overall intramolecular equilibrium constant $K_{\mathrm{I/tot}}$ [Eq. (18)][35,38,74,87] and the accessible stability enhancement $\log \Delta_{\mathrm{M/NP}}$, which is self-explaining [Eq. (17)], is given by Equations (18a) through (18e):[43,86]

$$\log \Delta_{\mathrm{M/NP}} = \log K^{\mathrm{M}}_{\mathrm{M(NP)_{exp}}} - \log K^{\mathrm{M}}_{\mathrm{M(NP)_{calc}}} \tag{17a}$$

$$= \log K^{\mathrm{M}}_{\mathrm{M(NP)}} - \log K^{\mathrm{M}}_{\mathrm{M(NP)_{op}}} \; (= \log \Delta) \tag{17b}$$

$$K_{\mathrm{I/tot}} = \frac{K^{\mathrm{M}}_{\mathrm{M(NP)}}}{K^{\mathrm{M}}_{\mathrm{M(NP)_{op}}}} - 1 = 10^{\log \Delta} - 1 \tag{18a}$$

$$= \frac{[\mathrm{M(NP)_{cl/tot}}]}{[\mathrm{M(NP)_{op}}]} \tag{18b}$$

$$= \frac{[\mathrm{M(NP)_{cl/O}}] + [\mathrm{M(NP)_{cl/O/N3}}]}{[\mathrm{M(NP)_{op}}]} \tag{18c}$$

$$= K_{\mathrm{I/O}} + K_{\mathrm{I/O/N3}} \cdot K_{\mathrm{I/O}} \tag{18d}$$

$$= K_{\mathrm{I/O}} (1 + K_{\mathrm{I/O/N3}}) \tag{18e}$$

At this point it is instructive to consider briefly the effect of substituents at C2 and C6 on metal-base interactions. The shift of the amino group from C6 in PMEA to C2 in 9-[(2-phosphonomethoxy)ethyl]-2-aminopurine (PMEA2AP)[44] relieves steric hindrance on the N7 site, but hinders M^{2+} coordination at N3 (see structures in Figure 1).[44] Accordingly, in

complexes with 9-[2-(phosphonomethoxy)ethyl]-2-amino-6-dimethylaminopurine (PME2A6DMAP)[46] the N3 site is blocked by the C2(NH_2) group and coordination at N7 is sterically hindered by the $N(CH_3)_2$ group at C6. Hence, in M(PME2A6DMAP) complexes only the 5-membered chelate as seen in Equilibrium (19)[45] forms; no isomers with metal ion-nucleobase interactions occur.[46]

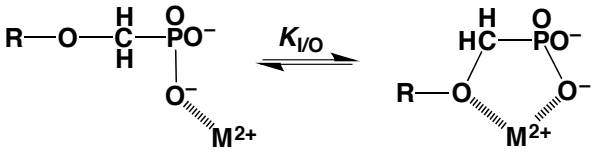

(19)

Considering the structural relationship between PMEA and HPMPA (Figure 1) we conclude from the summaries given in this section that for M(HPMPA) complexes (if at all) only the upper pathway seen in the Equilibrium Scheme (12) is of real relevance (see Section 2.7).

insert Figure 3 close to here

A quantitative evaluation regarding stability enhancements [Eq. (17)] is possible as indicated in Figure 3. The straight reference lines are based on the relationship between $\log K^{M}_{M(R\text{-}PO_3)}$ and $pK^{H}_{H(R\text{-}PO_3)}$ [Eq. (20)]:

$$\log K^{M}_{M(R\text{-}PO_3)} = m \cdot pK^{H}_{H(R\text{-}PO_3)} + b \qquad (20)$$

The slopes *m* and the intercepts *b* with the *y* axis are tabulated for all M^{2+} systems considered here.[38,66,73] The eight data points (empty circles) refer to simple phosph(on)ate systems (see legend of Figure 3), where R in R-PO_3 does not interact with M^{2+} (neither in a positive nor in a negative manner).

The data points for the M(NP) systems of $HPMPA^{2-}$/$PMEA^{2-}$ and $HPMP^{2-}$/PME^{2-} (Figure 1) are all above their reference lines proving an enhanced stability (Figure 3). Application of Equation (20) with the known parameters for *m* and *b*, and the $pK^{H}_{H(NP)}$ value of the ligand considered gives the log stability constant $\log K^{M}_{M(NP)_{op}}$, i.e., of the isomer in which M^{2+} is only coordinated to the phosphonate group [Eq. (19); species at the left]. Hence, the vertical dotted lines in Figure 3 correspond to the log $\Delta_{M/NP}$ values defined in Equation (17). Of course, the stability enhancements observed in Figure 3 and the values for log $\Delta_{M/NP}$ [Eq. (17)] represent the

total enhancement which involves all possible isomers. In Table 6 the results are assembled for the M(HPMPA) systems. Any breakdown into individual isomers has to occur in separate steps based on further arguments.

insert Table 6 close to here

2.7 Evaluation of the Stability Enhancements of the M(HPMPA) Complexes

From the stability enhancements seen in Figure 3 which correspond to the log $\Delta_{M/HPMPA}$ values [Eq. (17)] listed in Table 6 (column 4) it follows that next to the phosphonate group, at least in part other binding sites of $HPMPA^{2-}$ (see Figure 1) allowing chelate formation, must be involved. The *total* amount of closed species is given by Equation (21),

$$\% M(NP)_{cl/tot} = 100 \cdot K_{I/tot} / (1 + K_{I/tot}) \quad (21)$$

and the percentage of the open species (op) equals of course:

$$\% M(NP)_{op} = 100 \% - \% M(NP)_{cl/tot} \quad (22)$$

The potential metal ion-binding sites of $HPMPA^{2-}$ are the ether-oxygen of the $–CH_2–O–CH_2–PO_3^{2-}$ residue, the hydroxyl group of the $HO–CH_2–$ side chain and the N3 or N7 sites of the adenine moiety, the N7 site not being of relevance, as discussed. Furthermore, the N1 site cannot be reached by a metal ion coordinated at the phosphonate group.[35,38,85] To solve this rather complex problem we employ comparisons with the nucleobase-free $HPMP^{2-}$ and with the side-chain-free $PMEA^{2-}$. To this end we list in Table 7 the corresponding log $\Delta_{M/NP}$ values.

insert Table 7 close to here

From the differences $\Delta \log \Delta_{HPMPA–HPMP}$ follows directly the effect of the adenine residue on the stability of the complexes. It is apparent that this residue inhibits complexation of Ba^{2+}, Sr^{2+}, Ca^{2+}, Mg^{2+} and Mn^{2+}. Interestingly, the log $\Delta_{M/HPMPA}$ values (column 2) correspond for the mentioned metal ions to those of log $\Delta_{M/PMEA}$ (column 5). Furthermore, it has been concluded that for the complexes of Ba^{2+}, Sr^{2+}, and Ca^{2+} a significant portion of tridentate binding of the

$HPMP^{2-}$ ligand occurs; that is, formation degrees of about 30 % of the $M(HPMP)_{cl/O/OH}$ isomers are reached.[47] Evidently, with $HPMPA^{2-}$ such a type of chelate formation does not occur; most likely, the adenine residue hampers, due to its steric bulk, the formation of a species analogous to $M(HPMP)_{cl/O/OH}$. In contrast, from the differences listed in column 4 of Table 7 for the complexes with Ni^{2+} and Cu^{2+} it follows unequivocally that the adenine residue is involved in complex formation; for Zn^{2+} the situation is less clear from these data. These observations will be discussed further below in Section 2.8.

From the values listed in column 6 of Table 7, which follow from the differences of the log $\Delta_{M/NP}$ values of the complexes formed with $HPMPA^{2-}$ and $PMEA^{2-}$, one may estimate the effect of the hydroxyl group of the $HO–CH_2–$ side chain (Figure 1). All the differences are very small, that is, they are mostly zero within the error limits. There is possibly a small positive difference for the Δ log $\Delta_{HPMPA–PMEA}$ values in the case of the Ni^{2+} and Cu^{2+} complexes, but the values are so small that they do not justify to postulate the involvement of the hydroxyl group of $HPMPA^{2-}$, especially as there is no sign for such an interaction in the Ni^{2+} and Cu^{2+} complexes of $HPMP^{2-}$ as comparisons with the corresponding PME^{2-} complexes show (Table 7, column 7).[47] Consequently, we conclude that in all M(HPMPA) complexes the hydroxyl group does not participate in a significant manner in complex formation. Hence, in all instances, with the clear exception of Ni^{2+} and Cu^{2+} (and possibly Zn^{2+}), for which the adenine residue participates (see below in Section 2.8), there are only two isomeric complexes to be considered. That is, an open (op) species with a phosphonate coordination alone and a closed (cl) species involving the ether oxygen, i.e., Equilibrium (19) is of relevance. The formation degrees of these 5-membered chelates are already listed in column 6 of Table 6; they vary between about 20 and 70% demonstrating their importance.

2.8 Intramolecular Equilibria in the M(HPMPA) Complexes of Ni^{2+}, Cu^{2+}, and Zn^{2+}

As discussed before, for the $HPMPA^{2-}$ complexes of Ni^{2+}, Cu^{2+}, and possibly Zn^{2+} the complete upper pathway of the Equilibrium Scheme (12) is of relevance. This means, we have to deal with three isomeric species: (i) an open (op) isomer with a metal ion-phosphonate coordination only,

$M(HPMPA)_{op}$, (ii) a closed (cl) species, $M(HPMPA)_{cl/O}$, involving the ether-oxygen in a 5-membered chelate as seen in Equilibrium (19), and (iii) a tridentate chelate in which the 5- and a 7-membered ring is formed, the 7-membered one involving N3, $M(HPMPA)_{cl/O/N3}$ (see Figure 4 and also the ligand structure in Figure 1).

insert Figure 4 close to here

Analogous schemes involving three different isomers have been evaluated before;[38,47,85] therefore we will keep the following elaboration brief. The experimentally accessible stability constant [Eq. (5)] refers to the sum of all isomeric M(HPMPA) complexes [Eq. (16)] as discussed before in the context of the upper part of Equilibrium Scheme (12). Hence, Equations (13) through (18) can be applied. The corresponding results are summarized in Table 8.

insert Table 8 close to here

From the results in Table 8 it follows that all three isomers seen in the upper pathway of the Equilibrium Scheme (12) are of relevance, but it is also clear that in the three M^{2+}/$HPMPA^{2-}$ systems, that is, with $M^{2+} = Ni^{2+}$, Cu^{2+}, and Zn^{2+}, the $M(HPMPA)_{cl/O/N3}$ species are in fact the dominating isomers. Note that this indicates that under special conditions N3 can be an important metal ion binding site (see also Section 3).

3. Conclusions

Both HPMPA and PMEA are active antivirals,[88] albeit with different activity spectra. Whilst HPMPA can be considered as a broad-spectrum antiviral compound against DNA viruses, PMEA has only low activity against these. In turn, PMEA is active against retroviruses, whereas HPMPA is not.[89] Both compounds are active against herpes and pox viruses. HPMPA tends to be a better substrate for kinases than PMEA,[90] and its diphosphoryl derivative can act as alternative substrate for DNA polymerases,[17] a feat that is not possible for PMEApp.[20] The latter mechanistic differences are owed to the hydroxymethyl group present in HPMPA that renders it a closer structural analogue of dAMP.

However, in terms of ligand basicity (Table 1) and metal complex formation (Tables 2 and

7), the hydroxyl group in HPMPA does not affect the stability of protonated or metallated species; therefore the speciation of metal complexes with $HPMPA^{2-}$ is closely similar to that of $PMEA^{2-}$.[38] Both ligands form five-membered chelates to a significant extent [e.g., 31% for Mg(PMEA) and 24% for Mg(HPMPA)], which may impact substrate recognition by cellular enzymes.

As we have seen, N3 can be an important binding site, a fact that has been long overlooked because its basicity has been underestimated. It has recently been shown that N3 of adenosine possesses remarkable basic properties: The micro acidity constant $pk_{(N3)H}$ of *mono*protonated adenosine is 1.5 ± 0.3,[27] and in accord herewith the acyclic adenine-containing nucleotide analogues $PMEA^{2-}$ and $HPMPA^{2-}$ show the potential of (N3)-metal ion coordination. This is a fundamentally important observation, if one recalls that N3 is exposed to the solvent in the minor groove of DNA.[25]

The significant tendency of HPMPA, and by inference, its congeners including Tenofovir (= PMPA; see Introduction and Figure 1), to form complexes with essential metal ions including Mg^{2+} and Ca^{2+} warrants considering whether the formation of such complexes may play any role in the pharmacokinetics of acyclic nucleoside phosphonates (ANPs) beyond the direct interaction of the metal complexes with the respective enzymes, or indeed in the development of any observed side effects of these compounds. Notably, Antiretroviral Therapy seems to be an independent risk factor for developing osteoporosis, a consequence of disturbed calcium metabolism.[91] The exact causes and consequences for this well-documented association have remained unclear. More specifically, treatment with Tenofovir disoproxil has been associated with secondary hyperparathyroidism, a condition that can be a consequence of disturbed calcium metabolism, and in turn may lead to reduced bone mineral density and osteoporosis.[91] Although it can be estimated from pharmacokinetic data[92] that circulating levels of ANPs will not exceed tens of micromolar and thus will be outstripped by circulating calcium[93] by two to three orders of magnitude, the potential interactions of ANPs with, e.g., plasma calcium and their significance has never been investigated directly. Given that small molecules such as clioquinol and PBT2 (a second-generation 8-hydroxyquinoline analog) seem to profoundly affect zinc and copper distribution in brain despite their modest affinities,[94] it may be worth considering similar

mechanisms for phosphonates adversely affecting whole-body calcium distribution in patients.

4. Experimental Section

The free acid of (*S*)-9-[3-hydroxy-2-(phosphonomethoxy)propyl]adenine, i.e., $H_2(HPMPA)^{\pm}$ (Figure 1), was prepared as described.[41,95,96] The same lot had been used previously for the studies of the ternary Cu(Arm)(HPMPA) complexes,[39] where Arm = 2,2'-bipyridine or 1,10-phenanthroline. All the other reagents were the same as used before in related studies.[37,47] The ionic strength, *I*, was always adjusted at 25°C to 0.1 M with $NaNO_3$ (when needed).

The experiments with HPMPA were carried out exactly like those described for HPMPC,[47] that is, the experimental procedures, the concentrations, and the equipment used, as well as the calculation procedures, etc., employed.

However, a few points warrant emphasis:

(i) Because the applied pH scale is based on proton activity, the acidity constants determined are so-called practical, mixed, or Brønsted constants.[59,60] The negative logarithms of these constants given for aqueous solution (25°C; I = 0.1 M, $NaNO_3$) can be converted into the corresponding concentration constants by subtracting 0.02 from the pK_a values listed.[60] The measured stability constants of the metal ion complexes are, as usually, concentration constants.

(ii) The ligand concentration in the experiments was typically 0.3 mM and the M^{2+}:HPMPA ratios were for most metal ions 111:1 and 55.5:1 (see [47]). Due to solubility problems the Zn^{2+}:HPMPA ratios were only 28:1 and 14:1, and those for Cu^{2+}:HPMPA were 11.1:1 and 5.6:1. The calculated stability constants of the metal ion complexes showed no dependence on pH or on the excess of M^{2+}.

(iii) The final results given are in each case always the averages of at least seven independent pairs of titrations. One titration of such a pair was without ligand and this allowed to define the beginning of the hydrolysis of $M(aq)^{2+}$ (= hydroxo complex formation); at this point data collection for the calculation of the stability constant of a complex was stopped.

Acknowledgements

The support of this study by the Departments of Chemistry of the University of Basel and the University of Warwick is gratefully acknowledged.

Keywords: Acyclic nucleoside phosphonates · Antivirals · Isomeric equilibria · Metal ion complexes · Nucleotide analogues

References

[1] E. De Clercq, G. D. Li, *Clin. Microbiol. Rev.* **2016**, *29*, 695–747.

[2] a) E. De Clercq, *Med. Res. Rev.* **2013**, *33*, 1278–1303; b) E. De Clercq, *Biochem. Pharmacol.* **2011**, *82*, 99–109.

[3] E. De Clercq, A. Holý, I. Rosenberg, T. Sakuma, J. Balzarini, P. C. Maudgal, *Nature* **1986**, *323*, 464–467.

[4] E. De Clercq, J. Descamps, P. De Somer, A. Holý, *Science* **1978**, *200*, 563–565.

[5] https://www.ema.europa.eu/en/medicines/human/EPAR/vistide (accessed 16/01/2019).

[6] https://www.ema.europa.eu/en/medicines/human/orphan-designations/eu3161777 (accessed 16/01/2019).

[7] https://www.ema.europa.eu/en/medicines/human/EPAR/hepsera (accessed 16/01/2019).

[8] https://www.ema.europa.eu/en/medicines/human/EPAR/viread (accessed 16/01/2019).

[9] https://www.ema.europa.eu/en/medicines/human/EPAR/truvada (accessed 16/01/2019).

[10] S. Botros, S. William, L. Hammam, Z. Zidek, A. Holý, *Antimicrob. Agents Chemother.* **2003**, *47*, 3853–3858.

[11] E. Devries, J. G. Stam, F. F. J. Franssen, H. Nieuwenhuijs, P. Chavalitshewinkoon, E. De Clercq, J. P. Overdulve, P. C. Vandervliet, *Mol. Biochem. Parasitol.* **1991**, *47*, 43–50.

[12] R. Kaminsky, C. Schmid, Y. Grether, A. Holý, E. De Clercq, L. Naesens, R. Brun, *Trop. Med. Int. Health* **1996**, *1*, 255–263.

[13] P. Potmesil, M. Krecmerova, E. Kmonickova, A. Holý, Z. Zidek, *Eur. J. Pharmacol.* **2006**, *540*, 191–199.

[14] C. B. Hartline, K. M. Gustin, W. B. Wan, S. L. Ciesla, J. R. Beadle, K. Y. Hostetler, E. R. Kern, *J. Infect. Dis.* **2005**, *191*, 396–399.

[15] K. Y. Hostetler, K. A. Aldern, W. B. Wan, S. L. Ciesla, J. R. Beadle, *Antimicrob. Agents Chemother.* **2006**, *50*, 2857–2859.

[16] D. C. Quenelle, D. J. Collins, L. R. Pettway, C. B. Hartline, J. R. Beadle, W. B. Wan, K. Y. Hostetler, E. R. Kern, *Antiviral Res.* **2008**, *79*, 133–135.

[17] W. C. Magee, N. Valiaeva, J. R. Beadle, D. D. Richman, K. Y. Hostetler, D. H. Evans, *Antimicrob. Agents Chemother.* **2011**, *55*, 5063–5072.

[18] K. Toth, J. F. Spencer, B. L. Ying, A. E. Tollefson, C. B. Hartline, E. T. Richar, J. J. Fan, J. L. Lyu, B. A. Kashemirov, C. Harteg, D. Reyna, E. Lipka, M. N. Prichard, C. E. McKenna, W. S. M. Wold, *Antiviral Res.* **2018**, *153*, 1–9.

[19] Y. Kumaki, J. D. Woolcott, J. P. Roth, T. Z. McLean, D. F. Smee, D. L. Barnard, N. Valiaeva, J. R. Beadle, K. Y. Hostetler, *Antiviral Res.* **2018**, *158*, 122–126.

[20] W. C. Magee, D. H. Evans, *Antiviral Res.* 2012, *96*, 169–180.

[21] C. A. Blindauer, A. Holý, H. Dvořáková, H. Sigel, *J. Chem. Soc., Perkin Trans. 2* **1997**, 2353–2363.

[22] H. Schwalbe, W. Thomson, S. Freeman, *J. Chem. Soc., Perkin Trans. 1* **1991**, 1348–1349.

[23] R. Tribolet, H. Sigel, *Eur. J. Biochem.* **1987**, *163*, 353–363.

[24] R. B. Martin, Y. H. Mariam, *Met. Ions Biol. Syst.* **1979**, *8*, 57–124.

[25] K. Aoki, *Met. Ions Biol. Syst.* **1996**, *32*, 91–134.

[26] K. Aoki, K. Murayama, *Met. Ions Life Sci.* **2012**, *10*, 43–102.

[27] L. E. Kapinos, B. P. Operschall, E. Larsen, H. Sigel, *Chem. Eur. J.* **2011**, *17*, 8156–8164.

[28] G. Palu, S. Stefanelli, M. Rassu, C. Parolin, J. Balzarini, E. De Clercq, *Antiviral Res.* **1991**, *16*, 115–119.

[29] a) I. Votruba, R. Bernaerts, T. Sakuma, E. De Clercq, A. Merta, I. Rosenberg, A. Holý, *Mol. Pharmacol.* **1987**, *32*, 524–529; b) A. Merta, I. Votruba, J. Jindřich, A. Holý, T. Cihlář, I. Rosenberg, M. Otmar, T. Y. Herve, *Biochem. Pharmacol.* **1992**, *44*, 2067–2077.

[30] A. Holý, I. Votruba, A. Merta, J. Černý, J. Veselý, J. Vlach, K. Šedivá, I. Rosenberg, M. Otmar, H. Hřebabecký, M. Trávniček, V. Vonka, R. Snoeck, E. De Clercq, *Antiviral Res.* **1990**, *13*, 295–311.

[31] W. C. Magee, K. A. Aldern, K. Y. Hostetler, D. H. Evans, *Antimicrob. Agents Chemother.* **2008**, *52*, 586–597.

[32] E. De Clercq, *Biochem. Pharmacol.* **2007**, *73*, 911–922.

[33] J. Shelton, X. Lu, J. A. Hollenbaugh, J. H. Cho, F. Amblard, R. F. Schinazi, *Chem. Rev.* **2016**, *116*, 14379–14455.

[34] a) H. Sigel, *Pure Appl. Chem.* **1999**, *71*, 1727–1740; b) H. Sigel, A. Sigel, *J. Indian Chem. Soc.* **2000**, *77*, 501–509.

[35] a) H. Sigel, *Coord. Chem. Rev.* **1995**, *144*, 287–319; b) H. Sigel, *Chem. Soc. Rev.* **2004**, *33*, 191–200.

[36] a) H. Sigel, R. Griesser, *Chem. Soc. Rev.* **2005**, *34*, 875–900; b) H. Sigel, *Pure Appl. Chem.* **2004**, *76*, 375–388.

[37] R. B. Gómez-Coca, C. A. Blindauer, A. Sigel, B. P. Operschall, A. Holý, H. Sigel, *Chem. Biodivers.* **2012**, *9*, 2008–2034.

[38] H. Sigel, D. Chen, N. A. Corfù, F. Gregáň, A. Holý, M. Strašák, *Helv. Chim. Acta* **1992**, *75*, 2634–2656.

[39] C. A. Blindauer, R. Griesser, A. Holý, B. P. Operschall, A. Sigel, B. Song, H. Sigel, *J. Coord. Chem.* **2018**, *71*, 1910–1934.

[40] A. Holý, E. De Clercq, I. Votruba, *ACS Symp. Ser.* **1989**, *401*, 51–71.

[41] H. Dvořáková, A. Holý, I. Rosenberg, *Collect. Czech. Chem. Commun.* **1994**, *59*, 2069–2094.

[42] C. A. Blindauer, A. Holý, H. Sigel, *Collect. Czech. Chem. Commun.* **1999**, *64*, 613–632.

[43] A. Fernández-Botello, R. Griesser, A. Holý, V. Moreno, H. Sigel, *Inorg. Chem.* **2005**, *44*, 5104–5117 (Dedicated to the memory of the late Prof. Dr. Nityananda Saha, Professor of Chemistry at the University of Calcutta and Vice Chancellor of Kalyani University, India).

[44] A. Fernández-Botello, B. P. Operschall, A. Holý, V. Moreno, H. Sigel, *Dalton Trans.* **2010**, *39*, 6344–6354.

[45] A. Sigel, B. P. Operschall, H. Sigel, *Coord. Chem. Rev.* **2012**, *256*, 260–278.

[46] R. B. Gómez-Coca, A. Sigel, B. P. Operschall, A. Holý, H. Sigel, *Can. J. Chem.* **2014**, *92*, 771–780 (*CJC* issue in honor of A. B. P. (Barry) Lever).

[47] C. A. Blindauer, A. Sigel, B. P. Operschall, A. Holý, H. Sigel, *Inorg. Chim. Acta* **2018**,

472, 283–294.

[48] A. Holý, *Antiviral Res.* **2006**, *71*, 248–253.

[49] B. Song, A. Holý, H. Sigel, *Gazz. Chim. Ital.* **1994**, *124*, 387–392.

[50] O. Yamauchi, A. Odani, H. Masuda, H. Sigel, *Met. Ions Biol. Syst.* **1996**, *32*, 207–270.

[51] C. Meiser, B. Song, E. Freisinger, M. Peilert, H. Sigel, B. Lippert, *Chem. Eur. J.* **1997**, *3*, 388–398.

[52] A. Sigel, B. P. Operschall, H. Sigel, *J. Biol. Inorg. Chem.* **2014**, *19*, 691–703 (*JBIC* issue dedicated to the memory of Ivano Bertini).

[53] G. Kampf, L. E. Kapinos, R. Griesser, B. Lippert, H. Sigel, *J. Chem. Soc., Perkin Trans 2* **2002**, 1320–1327.

[54] M. Bastian, F. Gregáň, G. Liang, H. Sigel, *Z. Naturforsch.* **1993**, *48B*, 1279–1287.

[55] S. S. Massoud, H. Sigel, *Inorg. Chem.* **1988**, *27*, 1447–1453.

[56] H. Sigel, S. S. Massoud, R. Tribolet, *J. Am. Chem. Soc.* **1988**, *110*, 6857–6865.

[57] E. M. Bianchi, S. A. A. Sajadi, B. Song, H. Sigel, *Chem. Eur. J.* **2003**, *9*, 881–892.

[58] H. Sigel, C. P. Da Costa, B. Song, P. Carloni, F. Gregáň, *J. Am. Chem. Soc.* **1999**, *121*, 6248–6257.

[59] M. Bastian, H. Sigel, *J. Coord. Chem.* **1991**, *23*, 137–154 (*JCC* issue in honor of Prof. Dr. Arthur E. Martell on the occasion of his 75th birthday).

[60] H. Sigel, A. D. Zuberbühler, O. Yamauchi, *Anal. Chim. Acta* **1991**, *255*, 63–72.

[61] A. Fernández-Botello, A. Holý, V. Moreno, H. Sigel, *Polyhedron* **2003**, *22*, 1067–1076.

[62] H. Sigel, *Pure Appl. Chem.* **2004**, *76*, 1869–1886.

[63] R. B. Martin, *Science* **1963**, *139*, 1198–1203.

[64] C. A. Blindauer, "Untersuchungen zu Stabilität, Struktur und Rektivität von Metallionenkomplexen einiger antiviraler Nukleotid-Analoga", PhD thesis, University of Basel (Switzerland), 1998.

[65] a) R. K. O. Sigel, H. Sigel, *Met. Ions Life Sci.* **2007**, *2*, 109–180; b) R. K. O. Sigel, M. Skilandat, A. Sigel, B. P. Operschall, H. Sigel, *Met. Ions Life Sci.* **2013**, *11*, 191–274.

[66] H. Sigel, B. Song, *Met. Ions Biol. Syst.* **1996**, *32*, 135–205.

[67] H. Sigel, S. S. Massoud, N. A. Corfù, *J. Am. Chem. Soc.* **1994**, *116*, 2958–2971.

[68] G. Liang, H. Sigel, *Inorg. Chem.* **1990**, *29*, 3631–3632.

[69] a) H. Irving, R. J. P. Williams, *Nature* **1948**, *162*, 746–747; b) H. Irving, R. J. P. Williams, *J. Chem. Soc.* **1953**, 3192–3210.

[70] H. Sigel, D. B. McCormick, *Acc. Chem. Res.* **1970**, *3*, 201–208.

[71] H. Sigel, *Chem. Soc. Rev.* **1993**, *22*, 255–267.

[72] A. Saha, N. Saha, L.-n. Ji, J. Zhao, F. Gregáň, S. A. A. Sajadi, B. Song, H. Sigel, *J. Biol. Inorg. Chem.* **1996**, *1*, 231–238.

[73] H. Sigel, L. E. Kapinos, *Coord. Chem. Rev.* **2000**, *200–202*, 563–594.

[74] H. Sigel, *J. Indian Chem. Soc.* **1997**, *74*, 261–271 (P. Ray Award Lecture).

[75] B. Knobloch, A. Okruszek, H. Sigel, *Inorg. Chem.* **2008**, *47*, 2641–2648.

[76] N. A. Corfù, A. Sigel, B. P. Operschall, H. Sigel, *J. Indian Chem. Soc.* **2011**, *88*, 1093–1115 (*JICS* issue commemorating the 150th birth anniversary of Sir Prafulla Chandra Ray).

[77] L. E. Kapinos, H. Sigel, *Inorg. Chim. Acta* **2002**, *337*, 131–142 (*ICA* issue dedicated to Prof. Dr. Karl E. Wieghardt).

[78] L. E. Kapinos, A. Holý, J. Günter, H. Sigel, *Inorg. Chem.* **2001**, *40*, 2500–2508.

[79] a) R. B. Martin, *Met. Ions Biol. Syst.* **1996**, *32*, 61–89; b) H. Sigel, N. A. Corfù, L.-n. Ji, R. B. Martin, *Comments Inorg. Chem.* **1992**, *13*, 35–59.

[80] M. Bastian, H. Sigel, *Inorg. Chim. Acta* **1991**, *187*, 227–237.

[81] R. K. O. Sigel, H. Sigel, *Acc. Chem. Res.* **2010**, *43*, 974–984.

[82] A. Sigel, B. P. Operschall, H. Sigel, *Met. Ions Life Sci.* **2017**, *17*, 319–402.

[83] H. Sigel, R. B. Martin, *Chem. Soc. Rev.* 1994, *23*, 83–91.

[84] B. Knobloch, R. K. O. Sigel, B. Lippert, H. Sigel, *Angew. Chemie Int. Ed.* **2004**, *43*, 3793–3795.

[85] C. A. Blindauer, A. H. Emwas, A. Holý, H. Dvořáková, E. Sletten, H. Sigel, *Chem. Eur. J.*

1997, *3*, 1526–1536.

[86] R. B. Gómez-Coca, A. Holý, R. A. Vilaplana, F. González-Vílchez, H. Sigel, *Bioinorg. Chem. Appl.* **2004**, *2*, 331–352.

[87] R. B. Gómez-Coca, L. E. Kapinos, A. Holý, R. A. Vilaplana, F. González-Vílchez, H. Sigel, *J. Chem. Soc., Dalton Trans.* **2000**, 2077–2087.

[88] E. De Clercq, *Antiviral Res.* **2007**, *75*, 1–13.

[89] R. Pauwels, J. Balzarini, D. Schols, M. Baba, J. Desmyter, I. Rosenberg, A. Holý, E. De Clercq, *Antimicrob. Agents Chemother.* **1988**, *32*, 1025–1030.

[90] A. Merta, J. Veselý, I. Votruba, I. Rosenberg, A. Holý, *Neoplasma* **1990**, *37*, 111–120.

[91] S. Noe, C. Oldenbuettel, S. Heldwein, C. Wiese, A. von Krosigk, R. Pascucci, K. Ruecker, H. Jaeger, E. Wolf, *Horm. Metab. Res.* **2018**, *50*, 317–324.

[92] B. P. Kearney, J. F. Flaherty, J. Shah, *Clin. Pharmacokinet.* **2004**, *43*, 595-612.

[93] B. A. Dilena, L. Larsson, S. Öhman, in *Handbook on Metals in Clinical and Analytical Chemistry*, (Eds.: H. Seiler, A. Sigel, H.Sigel), Marcel Dekker Inc., New York and Basel, **1994**, pp. 299–310.

[94] P. A. Adlard, A. I. Bush, *Front. Psychiatry* **2012**, *3*, (article no. 15).

[95] A. Holý, I. Rosenberg, *Collect. Czech. Chem. Commun.* **1987**, 52, 2775–2791.

[96] A. Holý, *Collect. Czech. Chem. Commun.* **1993**, *58*, 649–674.

Table 1. Negative logarithms of the acidity constants [Equations (1) to (3)] for aqueous solutions of $H_3(HPMPA)^+$ (Figure 1), together with corresponding data of related systems for comparison (25 °C; I = 0.1 M, $NaNO_3$)[a,b]

No.	Protonated Species	pK_a for the site $P(O)(OH)_2$	$(N7)H^+$	$(N1)H^+$	$P(O)\bar{}_2(OH)$	Refs
1	$H(9MeA)^+$		(2.96 ± 0.10)[f]	4.10 ± 0.01		[53]
2	$H_2(HPMP)$	1.51 ± 0.06[c]			6.94 ± 0.01	[47]
3	$H_3(HPMPA)^+$	1.16 ± 0.10[c]		4.14 ± 0.01[h]	6.84 ± 0.01[h]	[49]
4	$H_2(PME)$	1.57 ± 0.15[d]			7.02 ± 0.01	[38,54]
5	$H_3(PMEA)^+$	1.22 ± 0.13[c]		4.16 ± 0.02	6.90 ± 0.01	[38,43]
6	$H(Ado)^+$		(2.15 ± 0.15)[g]	3.61 ± 0.03		[23,27]
7	$H_2(RibMP)$	0.81 ± 0.06[c]			6.24 ± 0.01	[55]
8	$H_3(AMP)^+$	0.4 ± 0.2[e]		3.84 ± 0.02	6.21 ± 0.01	[56,57]
9	$CH_3OP(O)(OH)_2$	1.1 ± 0.2			6.36 ± 0.01	[58]
10	$CH_3P(O)(OH)_2$	2.10 ± 0.03			7.51 ± 0.01[i]	[58]

[a] So-called practical, mixed or Brønsted constants, determined (mostly) by potentiometric pH titrations, are listed (see also 4. Experimental Section).[59,60]

[b] The error limits given are three times the standard error of the mean value (3σ) or the sum of the probable systematic errors, whichever is larger. The error limits of the derived data, in the present case partly in column three (estimates based on differences),[c] were calculated according to the error propagation after Gauss.

[c] Estimate based on the information given in ref.[43]

[d] Estimate;[61] see also ref.[43]

[e] Determined by ^{1}H NMR shift experiments.[23]

[f] This micro acidity constant reflects the basicity of N7 under conditions where N1 does not carry a proton; i.e., $pk^{N7\text{-}N1}_{H\cdot N7\text{-}N1}$ = 2.96 ± 0.10 holds for the species $^+$H·N7(9MeA)N1. For the macro acidity constant $pK^{H}_{H_2(9MeA)}$ = –0.64 ± 0.06 holds as measured by UV spectrophotometry.[53,62]

[g] Micro acidity constant reflecting the basicity of N7 (cf. [f]), i.e., $pk^{N7\text{-}N1}_{H\cdot N7\text{-}N1}$ = 2.15 ± 0.15 [27] holds for the species $^+$H·N7(Ado)N1. The macro acidity constant of $H_2(Ado)^{2+}$ is $pK^{H}_{H_2(Ado)}$ = –1.50 ± 0.15.[53] Note, a change of I from 0.1 to 0.5 M has no remarkable effect on the value.[27]

[h] These values[49] were confirmed by potentiometric pH titrations in the present study. By ^{1}H NMR shift measurements in D_2O and transformation of the results to H_2O as solvent[63] the following results were obtained: pK_a = 6.86 ± 0.11 [for $P(O)\bar{}_2(OH)$], 4.23 ± 0.08 [for $(N1)H^+$] and 1.27 ± 0.11 [for $P(O)(OH)_2$].[64]

[i] In ref.[38] pK_a = 7.53 ± 0.01 is given.

Table 2. Logarithms of the stability constants of the $M(H;HPMPA)^+$ [Equation (4)] and M(HPMPA) complexes [Equation (5)], together with the negative logarithms of the acidity constants of the protonated $M(H;HPMPA)^+$ species [Equations (6), (7)] as determined by potentiometric pH titrations (aq. sol.; 25°C; I = 0.1 M, $NaNO_3$)[a]

M^{2+}	log $K^{M}_{M(H;HPMPA)}$	log $K^{M}_{M(HPMPA)}$	p$K^{H}_{M(H;HPMPA)}$
Ba^{2+}	0.0 ± 0.5[b]	1.33 ± 0.03	5.5 ± 0.5
Sr^{2+}	0.0 ± 0.3	1.39 ± 0.04	5.45 ± 0.3
Ca^{2+}	0.1 ± 0.3	1.64 ± 0.03	5.3 ± 0.3
Mg^{2+}	0.1 ± 0.3	1.81 ± 0.03	5.1 ± 0.3
Mn^{2+}	0.6 ± 0.2	2.46 ± 0.02	4.98 ± 0.2
Co^{2+}	0.84 ± 0.11	2.37 ± 0.02	5.31 ± 0.11
Ni^{2+}	1.28 ± 0.10	2.55 ± 0.02	5.57 ± 0.10
Cu^{2+}	1.79 ± 0.22[c]	4.05 ± 0.04[c]	4.58 ± 0.22[c]
Zn^{2+}	1.43 ± 0.18[c]	2.85 ± 0.15[c,d]	5.42 ± 0.23[c]
Cd^{2+}	1.25 ± 0.05	3.01 ± 0.04	5.08 ± 0.06

[a] For the acidity constants of the protonated ligand, $H_3(HPMPA)^+$, see Table 1. For the error limits see footnote [b] of Table 1.

[b] Estimate; the formation degree of $Ba(H;HPMPA)^+$ was very low.

[c] Constants determined previously[49] are log $K^{Cu}_{Cu(H;HPMPA)}$ = 1.73 ± 0.12, log $K^{Cu}_{Cu(HPMPA)}$ = 4.04 ± 0.03, and p$K^{H}_{Cu(H;HPMPA)}$ = 4.53 ± 0.12, as well as log $K^{Zn}_{Zn(H;HPMPA)}$ = 1.2 ± 0.2, log $K^{Zn}_{Zn(HPMPA)}$ = 2.73 ± 0.10, and p$K^{H}_{Zn(H;HPMPA)}$ = 5.3 ± 0.2.

[d] Experiment hampered by precipitation; i.e., the pH range accessible to evaluation was restricted.

Table 3. Estimation of the micro stability constant of the $(H{\cdot}HPMPA{\cdot}M)^{+}$ isomer (upper pathway in the scheme of Figure 2) in aqueous solution at 25°C and I = 0.1 to 0.5 M[a]

M^{2+}	m_{av}[b]	log $K^{M}_{M(Ado)}$ [c]	$m_{av}\cdot\Delta\, pK_a$[d]	log $k^{M}_{H\cdot HPMPA\cdot M}$ [e]	$k^{M}_{H\cdot HPMPA\cdot M}$ [f]
Mn^{2+}	0.117 ± 0.065	0.04 ± 0.09	0.062 ± 0.035	0.50 ± 0.18	3.16 ± 1.31
Co^{2+}	0.126 ± 0.060	0.23 ± 0.05	0.067 ± 0.032	0.70 ± 0.16	5.01 ± 1.85
Ni^{2+}	0.158 ± 0.043	0.40 ± 0.05	0.084 ± 0.023	0.88 ± 0.16	7.59 ± 2.80
Cu^{2+}	0.394 ± 0.003	0.84 ± 0.04	0.209 ± 0.012	1.45 ± 0.16	28.18 ± 10.38
Zn^{2+}	0.194 ± 0.091	0.15 ± 0.04	0.103 ± 0.049	0.65 ± 0.16	4.47 ± 1.65
Cd^{2+}	0.212 ± 0.081	0.64 ± 0.03	0.112 ± 0.043	1.15 ± 0.16	14.13 ± 5.20

[a] For the error limits see footnote [b] of Table 1.

[b] Average of the slopes m of the straight lines obtained for log K versus pK_a plots for *o*-substituted pyridine-type ligands[77] as well as for benzimidazole-type ligands;[78] see also text in Section 2.4. The error limits are chosen such that the slopes m of the two straight lines for a given M^{2+} are covered.

[c] Log stability constant of $M(Ado)^{2+}$ complexes as determined by potentiometric pH titrations in aqueous solution at 25°C and I = 0.5 M ($NaNO_3$). Details to be published by L. E. Kapinos and H. Sigel; the same values are also given in refs.[81,82]

[d] See Equation (9).

[e] The logarithms of the micro stability constants (see Figure 2; upper part at the left) are calculated according to Equation (9). The first two terms of this equation are given above in columns 3 and 4. The charge effect of 0.40 ± 0.15 log units[38,56,59,80] reflects the effect of the difference in charge between $M(Ado)^{2+}$ and $(H{\cdot}HPMPA{\cdot}M)^{+}$, that is, in the first case the reaction takes place (see also text in Section 2.4) between M^{2+} and the neutral Ado whereas in the second case the reaction occurs with $(H{\cdot}HPMPA)^{-}$ (see structures in Figure 1). This value due to the charge effect is added to the sum of the two values given at the left in columns 3 and 4.

[f] These micro stability constants, which follow from the log values at the left, are needed for the evaluations summarized in Table 5.

Table 4. Summary of the microconstants defined in the equilibrium scheme of Figure 2[a]

M^{2+}	$pK^{H}_{H(HPMPA)} - \log K^{M}_{M(HPMPA)}$ [b]	$\log k^{M}_{H\cdot HPMPA\cdot M}$ [c]	$\log k^{M}_{H(M\cdot HPMPA)}$ [d]	$pk^{H}_{H\cdot HPMPA\cdot M}$ [e]	$pk^{H}_{H(M\cdot HPMPA)}$ [f]
Mn^{2+}	4.38 ± 0.02	0.50 ± 0.18	–0.09 ± 1.20[f]	4.88 ± 0.18	4.29 ± 1.20
Co^{2+}	4.47 ± 0.02	0.70 ± 0.16	0.28 ± 0.58[f]	5.17 ± 0.16	4.75 ± 0.58
Ni^{2+}	4.29 ± 0.02	0.88 ± 0.16	1.06 ± 0.20	5.17 ± 0.16	5.35 ± 0.20
Cu^{2+}	2.79 ± 0.04	1.45 ± 0.16	1.52 ± 0.43	4.24 ± 0.16	4.31 ± 0.43
Zn^{2+}	3.99 ± 0.15	0.65 ± 0.16	1.35 ± 0.22	4.64 ± 0.22	5.34 ± 0.27
Cd^{2+}	3.83 ± 0.04	1.15 ± 0.16	0.56 ± 0.66[f]	4.98 ± 0.16	4.39 ± 0.66

[a] For the error limits see footnote [b] of Table 1.

[b] The relevant acidity constant is $pK^{H}_{H(HPMPA)} = 6.84 \pm 0.01$ (Table 1; entry 3, column 6) and the values for $\log K^{M}_{M(HPMPA)}$ are listed in column 3 of Table 2; hence, the values in the above column 2 can be calculated.

[c] These micro stability constants (see at the left in the upper part of the equilibrium scheme in Figure 2) are from column 5 in Table 3.

[d] These micro stability constants are calculated with Equation (a) given in the lower part of Figure 2, by applying the log stability constants, $\log K^{M}_{M(H;HPMPA)}$, of column 2 in Table 2 and the log of the micro stability constants in column 5 of Table 3.

[e] These values follow from the closed circle in the upper pathway of the equilibrium scheme; the same is true for the lower pathway [see also Equation (c)].

[f] The error limits are so large because the difference is taken between two very similar values in the closed circle, e.g., in the case of Mn^{2+} between $K^{M}_{M(H;HPMPA)} = 3.98 \pm 1.83$ and $k^{M}_{H\cdot HPMPA\cdot M} = 3.16 \pm 1.31$, which amounts to $k^{M}_{H(M\cdot HPMPA)} = 0.82 \pm 2.25$ (and also to log $k^{Mn}_{H(Mn\cdot HPMPA)} = -0.09 \pm 1.20$ as given in column 4).

Table 5. Isomeric distribution and formation degree of the $(H{\cdot}HPMPA{\cdot}M)^{+}$ species with M^{2+} at the nucleobase residue (aq. sol.; 25°C; I = 0.1 M)[a]

M^{2+}	$K^{M}_{M(H;HPMPA)}$ [b]	$k^{M}_{H\cdot HPMPA\cdot M}$ [c]	$k^{M}_{H(M\cdot HPMPA)}$ [d]	R[e]	% $(H{\cdot}HPMPA{\cdot}M)^{+}$[f]
Mn^{2+}	3.98 ± 1.83	3.16 ± 1.31	0.82 ± 2.25	3.85	79 (ca. 100; 47)
Co^{2+}	6.92 ± 1.75	5.01 ± 1.85	1.91 ± 2.55	2.62	72 (99; 46)
Ni^{2+}	19.05 ± 4.39	7.59 ± 2.80	11.46 ± 5.21	0.66	40 (55; 25)
Cu^{2+}	61.66 ± 31.24	28.18 ± 10.38	33.48 ± 32.92	0.84	46 (63; 29)
Zn^{2+}	26.92 ± 11.16	4.47 ± 1.65	22.45 ± 11.28	0.20	17 (23; 11)
Cd^{2+}	17.78 ± 2.05	14.13 ± 5.20	3.65 ± 5.59	3.87	79 (ca 100; 50)

[a] For the error limits see footnote [b] of Table 1.

[b] These values follow from those given in column 2 of Table 2.

[c] These values are from the terminating column in Table 3.

[d] Calculated according to Equation (a) in Figure 2.

[e] See Equation (10).

[f] See Equation (11). The values in parentheses refer to the upper and lower limits, respectively, for % $(H{\cdot}HPMPA{\cdot}M)^{+}$ as they result from the use of the upper and lower limits for $k^{M}_{H\cdot HPMPA\cdot M}$ (above in column 3). The difference to 100% describes the formation degree of the $H(M{\cdot}HPMPA)^{+}$ species.

Table 6. Stability constant comparisons according to Equation (17) for the M(HPMPA) complexes between the experimentally measured (exp) and the calculated (calc) log stability constants, together with the resulting intramolecular equilibrium constants, $K_{I/tot}$ [Equation (18)], and the formation degrees of the total amount of chelated species, $M(HPMPA)_{cl/tot}$ (aq. sol.; 25°C; I = 0.1 M, $NaNO_3$)[a]

M^{2+}	log $K^{M}_{M(HPMPA)}$		log $\Delta_{M/HPMPA}$[d]	$K_{I/tot}$[e]	$\%(HPMPA)_{cl/tot}$[f]
	exp[b]	calc[c]			
Ba^{2+}	1.33 ± 0.03	1.22 ± 0.04	0.11 ± 0.05	0.29 ± 0.15	22 ± 9
Sr^{2+}	1.39 ± 0.04	1.29 ± 0.04	0.10 ± 0.06	0.26 ± 0.16	21 ± 10
Ca^{2+}	1.64 ± 0.03	1.53 ± 0.05	0.11 ± 0.06	0.29 ± 0.17	22 ± 10
Mg^{2+}	1.81 ± 0.03	1.69 ± 0.03	0.12 ± 0.04	0.32 ± 0.13	24 ± 7
Mn^{2+}	2.46 ± 0.02	2.31 ± 0.05	0.15 ± 0.05	0.41 ± 0.18	29 ± 9
Co^{2+}	2.37 ± 0.02	2.08 ± 0.06	0.29 ± 0.06	0.95 ± 0.28	49 ± 7
Ni^{2+}	2.55 ± 0.02	2.10 ± 0.05	0.45± 0.05	1.82 ± 0.35	65 ± 4
Cu^{2+}	4.05 ± 0.04	3.17 ± 0.06	0.88 ± 0.07	6.59 ± 1.26	87 ± 2
Zn^{2+}	2.85 ± 0.15	2.34 ± 0.06	0.51 ± 0.16	2.24 ± 1.20	69 ± 11
Cd^{2+}	3.01 ± 0.04	2.65 ± 0.05	0.36 ± 0.06	1.29 ± 0.34	56 ± 6

[a] For the error limits see footnote [b] of Table 1.

[b] From column 3 in Table 2.

[c] Calculated with the previously established parameters[35,38,66,73] for the reference-line equations [Eq. (20)] and $pK^{H}_{H(HPMPA)}$ = 6.84 ± 0.01 (Table 1, entry 3).

[d] See Equation (17).

[e] See Equation (18).

[f] See Equation (21).

Table 7. Comparison of the log $\Delta_{M/NP}$ values, which quantify according to Equation (17) any stability enhancement due to chelate formation for the complexes formed with $HPMPA^{2-}$, $HPMP^{2-}$, and $PMEA^{2-}$, allowing thus conclusions regarding the influence of the adenine residue and the hydroxyl group (aq. sol.; 25°C; I = 0.1 M, $NaNO_3$)[a]

M^{2+}	log Δ_{HPMPA}	log Δ_{HPMP}	Δ log $\Delta_{HPMPA-HPMP}$	log Δ_{PMEA}	Δ log $\Delta_{HPMPA-PMEA}$	Δ log $\Delta_{HPMP-PME}$[b]
Ba^{2+}	0.11 ± 0.05	0.26 ± 0.04	–0.15 ± 0.06	0.08 ± 0.06	0.03 ± 0.08	0.16 ± 0.06
Sr^{2+}	0.10 ± 0.06	0.22 ± 0.05	–0.12 ± 0.08	0.07 ± 0.05	0.03 ± 0.08	0.15 ± 0.07
Ca^{2+}	0.11 ± 0.06	0.31 ± 0.05	–0.20 ± 0.08	0.11 ± 0.07	0.00 ± 0.09	0.17 ± 0.07
Mg^{2+}	0.12 ± 0.04	0.21 ± 0.03	–0.09 ± 0.05	0.16 ± 0.05	–0.04 ± 0.06	–0.01 ± 0.04
Mn^{2+}	0.15 ± 0.05	0.28 ± 0.05	–0.13 ± 0.07	0.21 ± 0.08	–0.06 ± 0.09	0.01 ± 0.07
Co^{2+}	0.29 ± 0.06	0.33 ± 0.06	–0.04 ± 0.08	0.28 ± 0.07	0.01 ± 0.09	0.04 ± 0.08
Ni^{2+}	0.45 ± 0.05	0.25 ± 0.05	0.20 ± 0.07	0.30 ± 0.07	0.15 ± 0.08	0.06 ± 0.07
Cu^{2+}	0.88 ± 0.07	0.54 ± 0.07	0.34 ± 0.10	0.77 ± 0.07	0.11 ± 0.10	0.06 ± 0.10
Zn^{2+}	0.51 ± 0.16	0.43 ± 0.06	0.08 ± 0.17	0.30 ± 0.10	0.21 ± 0.19	0.09 ± 0.08
Cd^{2+}	0.36 ± 0.06	0.33 ± 0.05	0.03 ± 0.08	0.33 ± 0.06	0.03 ± 0.08	0.03 ± 0.07

[a] For the error limits see footnote [b] of Table 1. The values in the second column are from column 4 in Table 6, those in the 3rd and 5th column are from ref.[47] and refs[34,38], respectively. In addition, for example, log Δ_{HPMPA} should correctly be written as log $\Delta_{M/HPMPA}$ [see also Equation (17)], however, for reasons of clarity "M" is deleted in all expressions above.

[b] These values are from column 6 in Table 2 of ref.[47].

Table 8. Total stability enhancements, log $\Delta_{M/HPMPA}$ [Equation (17)], observed for the M(HPMPA) complexes together with the intramolecular equilibrium constants and the percentages of the three isomeric species [Equilibrium (12); upper part] involved in the M(HPMPA) complexes of Ni^{2+}, Cu^{2+}, and Zn^{2+} (aq. sol.; 25°C; I = 0.1 M, $NaNO_3$)[a]

M^{2+}	log $\Delta_{M/HPMPA}$[b]	$K_{I/tot}$	% $M(HPMPA)_{cl/tot}$[c]	% $M(HPMPA)_{op}$[d]	$K_{I/O}$[e]	$K_{I/O/N3}$[f]	% $M(HPMPA)_{cl/O}$[c]	% $M(HPMPA)_{cl/O/N3}$[g]
Ni^{2+}	0.45 ± 0.05	1.82 ± 0.33	65 ± 4	35 ± 4	0.38 ± 0.22	3.79 ± 2.91	13 ± 8	52 ± 9
Cu^{2+}	0.88 ± 0.07	6.59 ± 1.22	87 ± 2	13 ± 2	2.02 ± 0.49	2.26 ± 1.00	26 ± 8	61 ± 9
Zn^{2+}	0.51 ± 0.16	2.24 ± 1.19	69 ± 11	31 ± 11	0.95 ± 0.31	1.36 ± 1.47	29 ± 14	40 ± 18

[a] For the error limits see footnote [b] of Table 1.

[b] Values taken from column 4 in Table 6. The use of these log $\Delta_{M/HPMPA}$ values for the calculation of $K_{I/tot}$ [Equation (18)] provides the same $K_{I/tot}$ values, but slightly different error limits than those given in Table 6 (column 5), which are based on log K_{exp} and log K_{calc}. Note, this has no effect on the values (including the error limits) calculated for % $M(HPMPA)_{cl/tot}$.

[c] Analogous to Equation (21).

[d] % $M(HPMPA)_{op}$ = 100% – % $M(HPMPA)_{cl}$ [Equation (22)].

[e] These values are from Table 6 (column 3) of ref.[44]; they refer to systems in which only the 5-membered chelate can form.

[f] Calculated with Equation (18).

[g] These values follow from % $M(HPMPA)_{cl/O/N3}$ = % $M(HPMPA)_{cl/tot}$ – % $M(HPMPA)_{cl/O}$. They can also be calculated analogous to Equation (21), but then the errors are understandably larger.

Legends for the Figures

Figure 1. Chemical structures of acyclic nucleoside phosphonates, that is, of the dianions of 9-[2-(phosphonomethoxy)ethyl]adenine ($PMEA^{2-}$) and (*S*)-9-[3-hydroxy-2-(phosphonomethoxy)propyl]adenine ($HPMPA^{2-}$) together with the structures of the nucleobase-free derivatives (phosphonomethoxy)ethane (PME^{2-} = (ethoxymethyl)phosphonate) and (*R*)-hydroxy-2-(phosphonomethoxy)propane ($HPMP^{2-}$). It is assumed that the orientation of $HPMPA^{2-}$ corresponds to the one observed for $PMEA^{2-}$ in solution[21] and in the solid state,[22] which resembles the *anti* conformation of the parent nucleotide, that is, adenosine 5'-monophosphate (AMP^{2-}).[23–26] AMP^{2-}, as well as the structures of 9-methyladenine (9MeA) and adenosine (Ado; also shown in its dominating *anti* conformation[27]) are given for comparison. (*R*)-9-[2-(phosphonomethoxy)propyl]adenine (PMPA; Tenofovir) lacks the 3-hydroxyl group present in HPMPA. All charged five compounds in the figure are also abbreviated as NP^{2-} = nucleoside phosph(on)ate derivative.

Figure 2. Equilibrium scheme for the reaction M^{2+} + H(HPMPA)$^{-}$ to M(HPMPA) + H^{+} which is shown in the upper part of the figure for Ni^{2+} as an example. In the lower part the interrelations between the macro- and microconstants are given in a general manner for M^{2+} [Eqs (a), (b), and (c)]. The equilibrium scheme shows the interrelation for the monoprotonated isomers of $Ni(H;HPMPA)^{+}$, written as $(H{\cdot}HPMPA{\cdot}Ni)^{+}$, with the metal ion at the adenine residue and the proton at the phosphonate group (upper pathway) and $H(Ni{\cdot}HPMPA)^{+}$ with both Ni^{+} and H^{+} at the phosphonate group (lower pathway; see text in Section 2.4). Also shown are the other species in equilibrium with $(H{\cdot}HPMPA{\cdot}Ni)^{+}$ and $H(Ni{\cdot}HPMPA)^{+}$. The arrows indicate the directions for which the constants are defined. The macroconstants are from Tables 1 and 2; the microconstants were derived by applying Equations (a), (b), and (c), together with the assumptions described in the text (Table 3). Further evaluations (Table 4) provide finally the ratio *R* and the percentages of the isomers of the monoprotonated complexes (Table 5).

Figure 3. Evidence for an enhanced stability of some M(HPMPA) (●) complexes in comparison

with those of the corresponding M(PMEA) (⊗), M(HPMP) (◆), and M(PME) (△) species [all abbreviated as M(NP)], based on the relationship between log $K^{M}_{M(R\text{-}PO_3)}$ and $pK^{H}_{H(R\text{-}PO_3)}$ for M(R-PO_3) complexes (○) of some simple phosphate monoester and phosphonate ligands (R-PO_3^{2-}): 4-nitrophenyl phosphate ($NPhP^{2-}$), phenyl phosphate (PhP^{2-}), uridine 5'-monophosphate (UMP^{2-}), D-ribose 5-monophosphate ($RibMP^{2-}$), thymidine [= 1-(2'-deoxy-β-D-ribofuranosyl)thymine] 5'-monophosphate ($dTMP^{2-}$), *n*-butyl phosphate (BuP^{2-}), methanephosphonate (MeP^{2-}), and ethanephosphonate (EtP^{2-}) (from left to right). The least-squares lines [Equation (20)][38,66,73] are drawn through the corresponding 8 data sets (○) taken from ref.[55] for the phosphate monoesters and from ref.[38] for the phosphonates. The points due to the equilibrium constants for the M^{2+}/HPMPA (●) systems are based on the values listed in Tables 1 and 2; those for the M^{2+}/PMEA systems (⊗) are from ref.[38], for the M^{2+}/HPMP systems (◆) from ref.[47], and those for the M^{2+}/PME systems (△) from ref.[38]. The vertical (broken) lines emphasize the stability differences based on the reference lines; they equal log $\Delta_{M/NP}$ as defined in Equation (17), for the M(NP) complexes in general. All the plotted equilibrium constants refer to aqueous solutions at 25°C and I = 0.1 M ($NaNO_3$).

Figure 4. Possible structure of a tridentate chelate with Cu^{2+} as central ion in a square planar geometry, involving the phosphonate group, the ether oxygen, and N3 of the adenine ring. Carbon atoms are shown in grey, nitrogen in blue, oxygens in red, phosphorus in magenta, and copper in cyan. Potential axial water ligands and all hydrogen atoms are omitted for clarity. The model was generated in Chem3D Pro v. 17, with customized restraints for distances, angles, and dihedral angles, some of which were extracted from the Cambridge Structural Database.

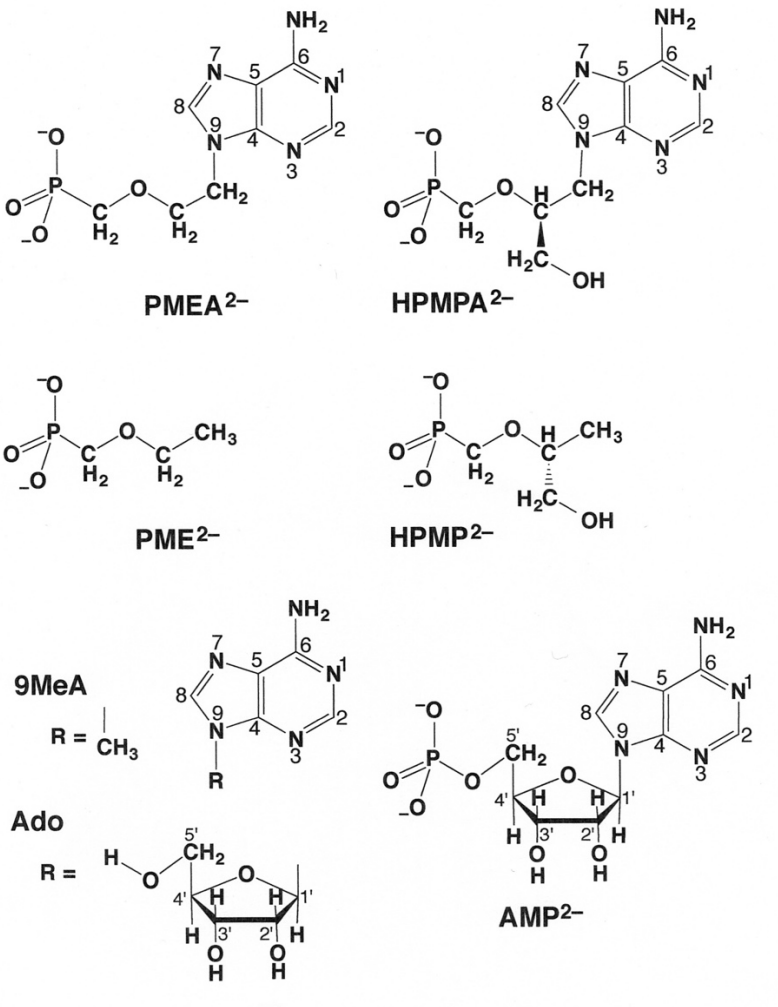

Figure 1

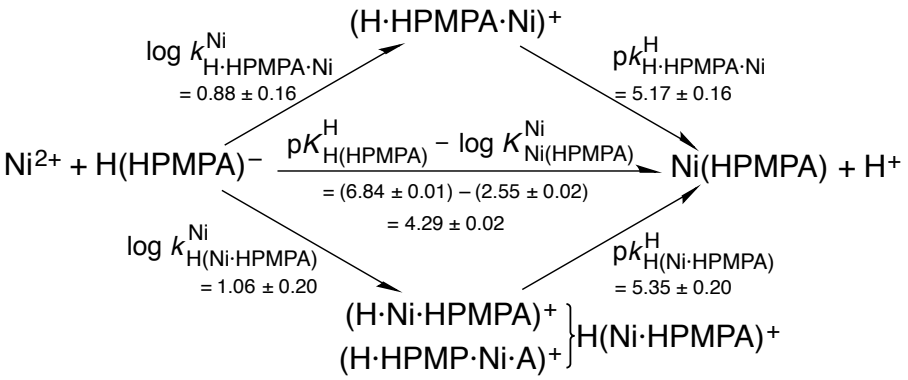

(a) $$K^{M}_{M(H;HPMPA)} = k^{M}_{H\cdot HPMPA\cdot M} + k^{M}_{H(M\cdot HPMPA)}$$

(b) $$\frac{1}{K^{H}_{M(H;HPMPA)}} = \frac{1}{k^{H}_{H\cdot HPMPA\cdot M}} + \frac{1}{k^{H}_{H(M\cdot HPMPA)}}$$

(c) $$K^{M}_{M(HPMPA)} \cdot K^{H}_{H(HPMPA)} = k^{M}_{H\cdot HPMPA\cdot M} \cdot k^{H}_{H\cdot HPMPA\cdot M} = k^{M}_{H(M\cdot HPMPA)} \cdot k^{H}_{H(M\cdot HPMPA)}$$

Figure 2

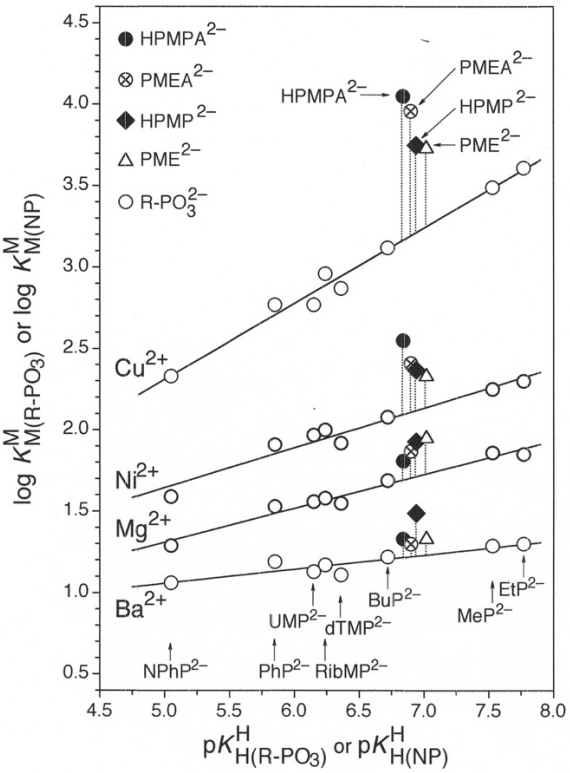
HPMPA2–
PMEA2–
HPMP2–
PME2–
R-PO32–
Cu2+
Ni2+
Mg2+
Ba2+
NPhP2–
UMP2–
PhP2–
dTMP2–
RibMP2–
BuP2–
MeP2–
EtP2–
log KM M(R-PO3) or log KM M(NP)
pKH H(R-PO3) or pKH H(NP)

Figure 3

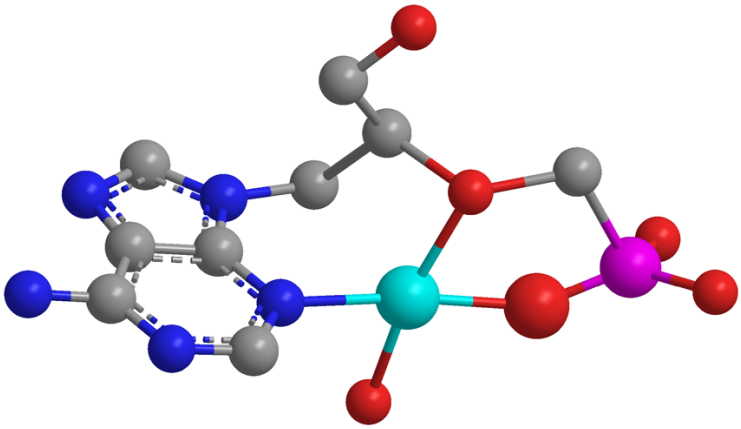

Figure 4

For the TOC

Antiviral Nucleotide Analogues

Metal-Coordinating Properties in Aqueous Solution of the Antivirally Active Nucleotide Analogue (*S*)-9-[3-Hydroxy-2-(phosphonomethoxy)propyl]adenine (HPMPA). Quantification of Complex Isomeric Equilibria

Claudia A. Blindauer, Antonín Holý, Bert P. Operschall, Astrid Sigel, Bin Song, and Helmut Sigel

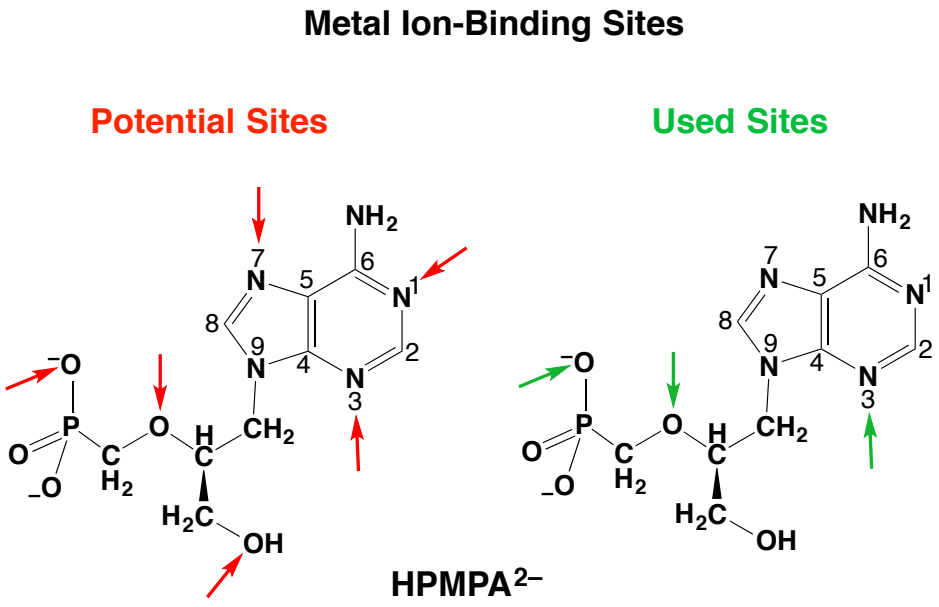

The primary binding site is the phosphonate group which forms with the ether O a 5-membered chelate, $M(HPMPA)_{cl/O}$. With varying formation degrees this intramolecular equilibrium holds for all metal ions studied. However, with Ni^{2+}, Cu^{2+}, and Zn^{2+} a further interaction is possible, that is, with N3 a 7-membered chelate is formed, $M(HPMPA)_{cl/O/N3}$.

Figure for the TOC

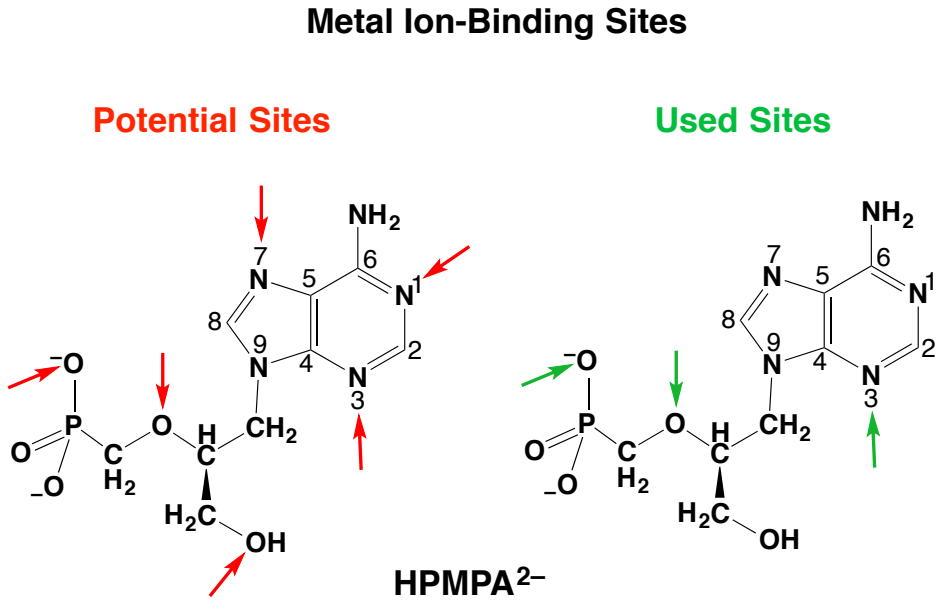

Text for the TOC

The primary binding site is the phosphonate group which forms with the ether O a 5-membered chelate, $M(HPMPA)_{cl/O}$. With varying formation degrees this intramolecular equilibrium holds for all metal ions studied. However, with Ni^{2+}, Cu^{2+}, and Zn^{2+} a further interaction is possible, that is, with N3 a 7-membered chelate is formed, $M(HPMPA)_{cl/O/N3}$.